ADVANCED OPTICAL MATERIALS
www.advopticalmat.de

Diffusion-Free Intramolecular Triplet–Triplet Annihilation Contributes to the Enhanced Exciton Utilization in OLEDs

Sara Mattiello, Andrew Danos, Kleitos Stavrou, Alessandra Ronchi, Roman Baranovski, Domenico Florenzano, Francesco Meinardi, Luca Beverina, Andrew Monkman, and Angelo Monguzzi**

Triplet–triplet annihilation (TTA), or triplet fusion, is a biexcitonic process in which two triplet-excited molecules can combine their energy to promote one into an excited singlet state. To alleviate the dependence of the TTA rate and yield on triplet diffusion in both solid and solution environments, intramolecular TTA (intra-TTA) has been recently proposed in conjugated molecular systems able to hold multiple triplet excitons simultaneously. Developing from the previous demonstration of TTA performance enhancement in sensitized upconversion solutions, here similar improvements in triplet harvesting in solid-state films are reported under electrical excitation in organic light emitting diodes (OLEDs). At low dye concentration and low current densities, the intra-TTA active OLED shows a +40% improved external quantum efficiency with respect to the reference device, and a TTA spin-statistical factor f^{4DPA} of 0.4, close to that determined in fluid solution for the individual chromophore (0.45). These results therefore indicate the utility of this molecular design strategy across a wider range of TTA applications, and with particular utility in the further development of low-power TTA-enhanced OLEDs.

1. Introduction

TTA, or triplet fusion, is a fundamentally interesting multi-excitonic process in which two triplet-excited molecules can combine their energy to promote one into an excited singlet state. In contrast to other mechanisms of generating emission from triplet states, such as phosphorescence or thermally activated delayed fluorescence (TADF),[1] the TTA and subsequent singlet emission can be both exothermic and spin-allowed, and remove the need for very high triplet energy host materials specifically for blue electroluminescence.[2] Considering the crucial role of triplet management in supporting advanced photonics and semiconductor applications, this function makes TTA a center piece of current organic electronics research, in areas as diverse as solar energy harvesting,[3] photocatalysis,[4] biological imaging,[5] 3D printing,[6] and optogenetics.[7]

Currently, the majority of TTA research is focused on sensitized upconversion for photovoltaic enhancement, in which sub-bandgap solar photons can be absorbed, combined, and re-radiated to a photovoltaic module. Enhancement by an upconversion layer allows circumvention of the Shockley-Queisser limit, which otherwise caps energy conversion of a single-bandgap device to approximately 30%.[8] Aside from photovoltaic applications, TTA is also important for triplet management in OLEDs.[9] In this context excitons are formed from uncorrelated electron and hole pairs in a ratio of 1:3 singlet:triplet. Without further intervention these triplet excitons are typically non-emissive, limiting the internal quantum efficiency (IQE) of such devices to 25%. While materials with triplet harvesting properties such as organometallic phosphors or those capable of TADF certainly exist, for various reasons these classes of materials have struggled to achieve high efficiency and device longevity at blue color coordinates—crucial for display and lighting applications.[2a,10] Hence, although the pairwise conversion of triplet excitons to singlets by TTA is only able to achieve a lower theoretical maximum IQEs of ≈63%,[11] such materials remain dominant in commercial OLEDs because of their as-yet unmatched device stability.

Despite the importance of TTA in a range of applications, only a relatively small group of TTA-active emitters are commonly investigated in academic settings.[12] For blue emission relevant to OLEDs, this is typically limited to derivatives of diphenyl

S. Mattiello, A. Ronchi, D. Florenzano, F. Meinardi, L. Beverina, A. Monguzzi
Dipartimento di Scienza dei Materiali
Università degli Studi Milano-Bicocca
via R. Cozzi 55, Milano 20125, Italy
E-mail: angelo.monguzzi@unimib.it

A. Danos, K. Stavrou, R. Baranovski, A. Monkman
Department of Physics
Durham University
Durham DH13LE, UK
E-mail: andrew.danos@durham.ac.uk

The ORCID identification number(s) for the author(s) of this article can be found under https://doi.org/10.1002/adom.202401597

© 2024 The Author(s). Advanced Optical Materials published by Wiley-VCH GmbH. This is an open access article under the terms of the Creative Commons Attribution License, which permits use, distribution and reproduction in any medium, provided the original work is properly cited.

DOI: 10.1002/adom.202401597

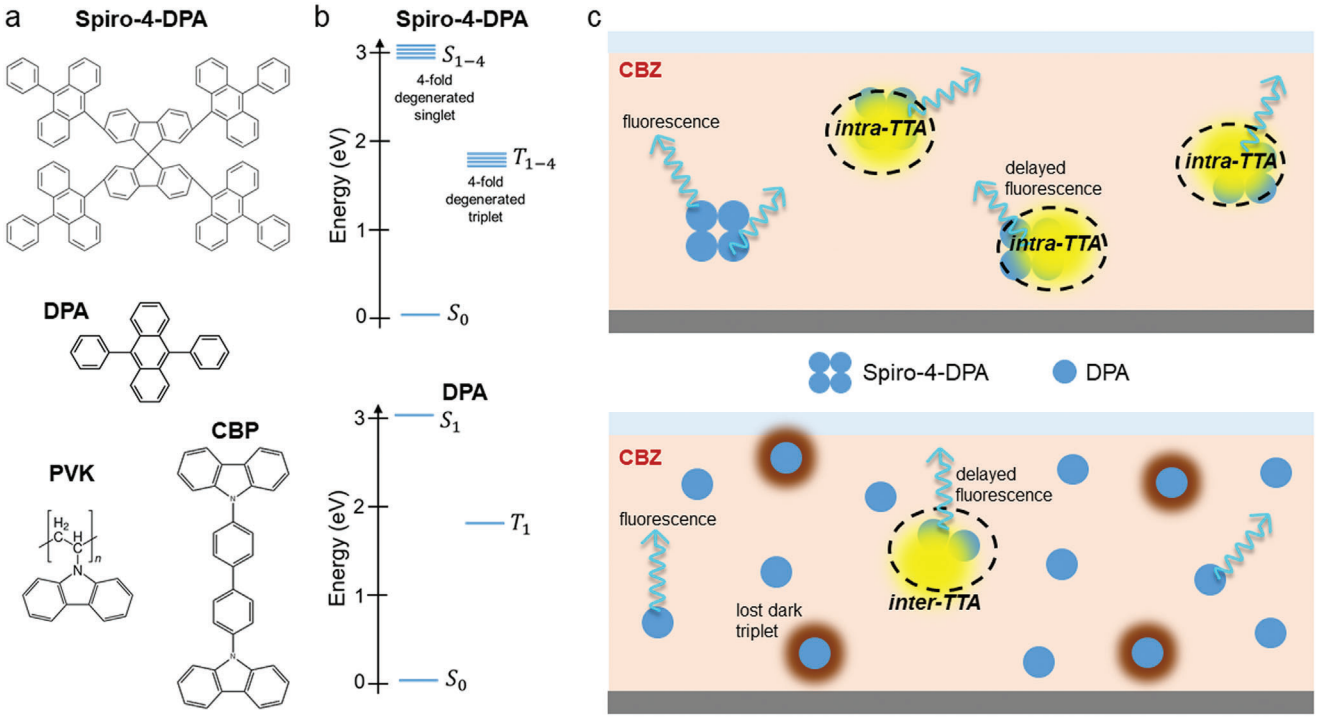

Figure 1. a) Molecular structure of the conjugated fluorophores 2,2′,7,7′-tetrakis(10-phenyl-anthracen-9-yl) 9,9′-spirobifluorene (spiro-4-DPA) and 9,10-diphenlyanthrnacene (DPA) employed to fabricate blue emitting films in polyvinylcabazole (PVK) or 4,4′-bis(N-carbazolyl)-1,1′-biphenyl (CBP). b) Ground state electronic energies of the employed dyes. c) Sketch of the OLED emissive layer with intramolecular triplet–triplet annihilation (intra-TTA) occurring in the spiro-4-DPA systems that produces additional blue photons, and DPA system where triplet harvesting only occurs through intermolecular TTA (inter-TTA). Upon the generation of the same total number of excitons with a singlet to triplet ratio 1:3, the intra-TTA is enabled even at low excitons densities because triplet excitons constantly migrate throughout the OLED sites, allowing double-capture processes on the same spiro-4-DPA. Conversely, for DPA molecules inter-TTA can happen only between nearby molecules thus leading to losses for triplet excitons on isolated chromophores.

anthracene (DPA) and perylene, with wider innovation in the chemical groups or structures somewhat rare.[13,14] Moreover, reflecting the popularity of sensitized upconversion applications, TTA is also most commonly investigated in solutions, while achieving and measuring TTA in the solid state is extremely challenging due to the low mobility of molecular excitons[15,16] and difficulty in managing molecular aggregation at the necessary high chromophore concentrations of films. In contrast, investigation of TTA in OLED contexts demands the use of solid films, but is also somewhat simplified by the possibility of direct electrical formation of triplet excitons—removing the need for doping with separate triplet sensitizer species to enable optical excitation.

In both solids and in solution though, TTA relies on either molecular or excitonic diffusion to bring together the prerequisite triplet pair. Pair formation can have a statistically limited probability for successfully going on to generate singlet excitons, and is typically rate limiting in the overall TTA process. Consequently, significant research effort has gone towards developing new materials that can sidestep this limitation. For example, confinement of both the optically active components in colloidal nanostructures[17] or nanocrystals[18] can increase the effective concentrations of excitons and therefore accelerate pair forming collisions. Developing multi-chromophore materials is also a recently popular approach, with covalent bonding in some cases holding the TTA-active chromophore pair permanently in favorable orientations for spin conversion.[19,20]

Exploiting this approach further, recently intra-TTA in the branched conjugated acceptor 2,2′,7,7′-tetrakis(10-phenyl-anthracen-9-yl)-9,9′-spirobifluorene (spiro-4-DPA) was demonstrated. As shown in **Figure 1a**, this emitter consists of four chemically anchored but energetically decoupled anthracene-like branches. Thanks to its capacity to hold up to four triplet excitons simultaneously (Figure 1b), this material was shown to undergo more efficient TTA at low concentrations and low excitation densities, as it can undergo diffusion-free intra-TTA after acquiring a second triplet exciton from the sensitizer.[21] Developing from this previous demonstration of performance enhancement in sensitized solution TTA upconversion systems, here we report similar improvements in triplet harvesting by solid-state films under electrical excitation in OLEDs. At low dye concentration and low current densities when diffusion-mediated intermolecular TTA is hindered, thanks to the intra-TTA contribution the spiro-4-DPA based OLEDs shows +40% improved EQE with respect to the reference DPA-based device, for which only intermolecular TTA (inter-TTA) can contribute to triplet harvesting as shown in Figure 1c. By modelling the relative OLED performance we arrive at a fitted spin-statistical factor for spiro-4-DPA (f^{4DPA}) of 0.4, which is close to the value for unmodified DPA in fluid solution (0.45), indicating efficient TTA events within the multi-chromophore material. These results therefore establish the utility of this molecular design strategy across a wider range of TTA applications, and with

© 2024 The Author(s). Advanced Optical Materials published by Wiley-VCH GmbH

21951071, 0, Downloaded from https://onlinelibrary.wiley.com/doi/10.1002/adom.202401597 by Universita Milano Bicocca, Wiley Online Library on [23/10/2024]. See the Terms and Conditions (https://onlinelibrary.wiley.com/terms-and-conditions) on Wiley Online Library for rules of use; OA articles are governed by the applicable Creative Commons License

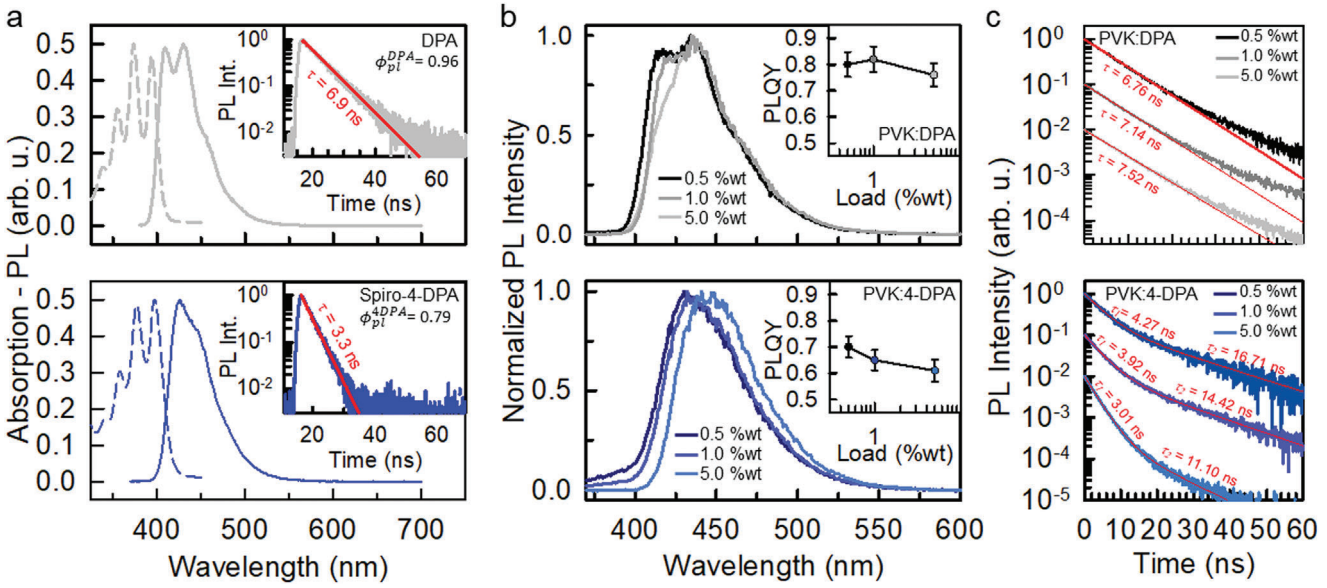

Figure 2. a) Spiro-4-DPA versus DPA absorption and photoluminescence (PL) spectra in THF diluted solution (10^{-5} M). The inset shows the PL intensity decay in time recorded at the PL maximum peak. b) PL of spiro-4-DPA in PVK films at different doping levels under 340 nm excitation. The inset reports thecorresponding PL quantum yield. c) PL intensity decay in time recorded at 440 nm for the PVK:DPA (top) and PVK:4-DPA (bottom) films series under pulsed excitation at 340 nm. Solid lines are the fit of data with single-exponential or multi-exponential decay functions.

particular utility in the further development of TTA-enhanced OLEDs.

2. Results and Discussion

The conjugated fluorophore spiro-4-DPA has been synthesized by a micellar catalyzed Suzuki–Miyaura coupling.[21] The system has been designed to allow the simultaneous coexistence of more than one independent triplet molecular exciton. When one of the equivalent triplets is populated, the remaining chromophores can host a second exciton, thus accommodating simultaneously two triplets on the same molecule in close proximity, and enabling their localized interaction and fast annihilation by intra-TTA (Figure S1, Supporting Information). Notably, this is possible because the center-to center distance between anthracene branches in the spiro-4-DPA system is as large as 1.1 nm, thus allowing short-range interactions such as Dexter transfer between the conjugated branches as well as TTA.[21] The system shows a remarkable stability, with no sign of thermal degradation upon heating up to 500 °C (Figure S2, Supporting Information). **Figure** 2a shows the photoluminescence properties of the spiro-4-DPA versus the reference DPA fluorophore in dilute THF. The spiro-4-DPA shows a slightly red-shifted absorption spectrum onset, peaked at 397 nm, indicating limited direct conjugation of chromophores across the spiro bridge.[22] The emission properties are also very similar between both materials, with spiro-4-DPA showing a bright blue photoluminescence peaked at 424 nm, high photoluminescence quantum yield ϕ_{pl}^{4DPA} of 0.79, and rapid fluorescence with lifetime of 3.2 ns (compared to 440 nm, 0.96, and 6.9 ns for DPA). The energy of the highest occupied molecular orbital (HOMO) and lowest unoccupied molecular orbital (LUMO) electronic levels of the spiro-4-DPA and DPA dyes have been estimated by combining cyclic voltammetry and optical absorption experiments (Section S3, Supporting Information), which gives again very similar results (Figures S3 and S4, Supporting Information).

Moving towards OLED applications, Figure 2 shows the photoluminescence spectra of solid films of polyvinylcabazole (PVK) loaded with 0.5, 1, or 5 wt% of spiro-4-DPA or DPA. PVK is a conductive polymer with good film-forming properties, which is sometimes used directly as a host material in solution-processed devices. PVK also provides a chemical environment for dopants analogous to evaporable OLED hosts such as 4,4′-bis(N-carbazolyl) 1,1′-biphenyl (CBP). At the higher concentrations employed, the emission spectrum from the PVK:DPA films shows some redshift. Considering the almost constant ϕ_{pl}^{DPA}= 0.76 ± 0.06 (Figure 2b, inset) and fluorescence lifetime $\tau \approx 7$ ns (Table S1, Supporting Information), we can ascribe the redshift to a trivial inner filter effect. The PVK:spiro-4-DPA series also shows a redshift in the photoluminescence spectrum as the dye concentration increases. In this case, we observe a corresponding slight decrease in the ϕ_{pl}^{4DPA}= 0.61 ± 0.08 and acceleration of the emission lifetime (with an additional ≈10 ns component) that suggests some aggregation formation in this material. While this evidence of enhanced aggregate formation in spiro-4-DPA films is surprising considering the similar chemical structures and four-fold lower molar concentration in the comparable films (determined from equal wt% doping, but different molecular masses), the ϕ_{pl} remain similar and assist in later interpretation of OLED performance.

Moving to actual OLEDs, evaporated devices were exclusively pursued in order to limit the deleterious effects of molecular aggregation that are commonly observed in TTA films,[23] and

© 2024 The Author(s). Advanced Optical Materials published by Wiley-VCH GmbH

21951071, 0, Downloaded from https://onlinelibrary.wiley.com/doi/10.1002/adom.202401597 by Universita Milano Bicocca, Wiley Online Library on [23/10/2024]. See the Terms and Conditions (https://onlinelibrary.wiley.com/terms-and-conditions) on Wiley Online Library for rules of use; OA articles are governed by the applicable Creative Commons License

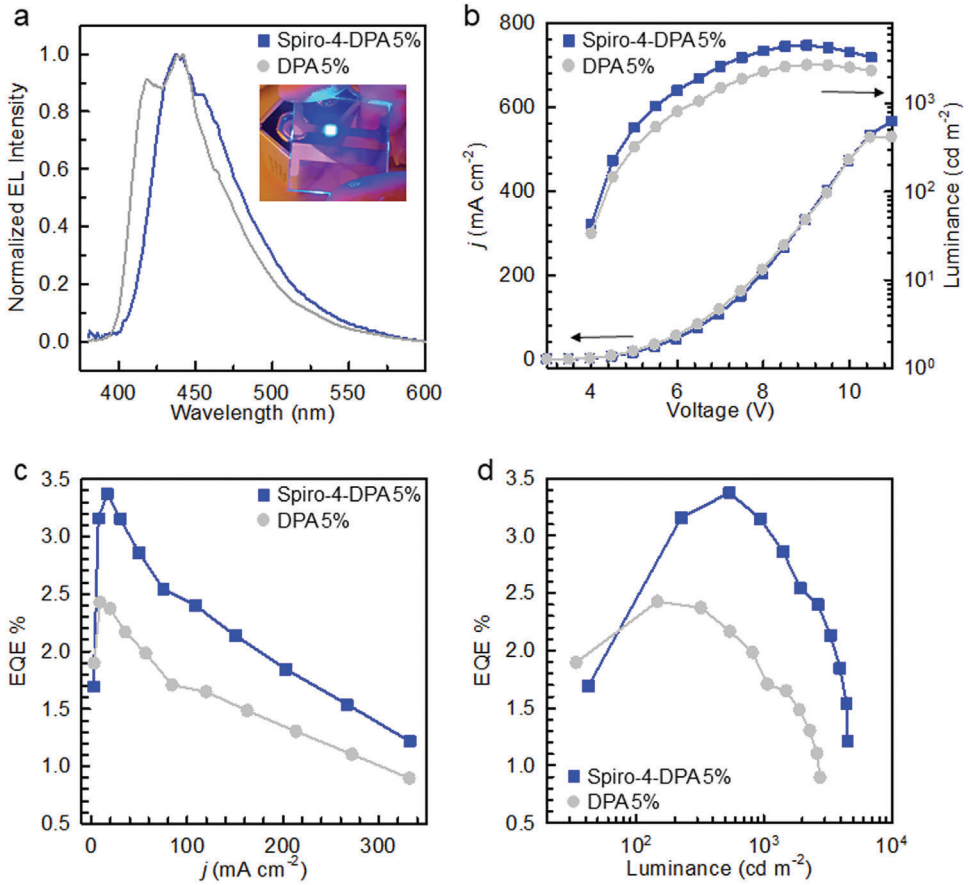

Figure 3. a) Electroluminescence (EL) spectra of the spiro-4-DPA and DPA (5 vol% in CBP) OLED devices at 5.5 V applied voltage. b) Current density and luminance of the investigated devices as a function of the applied voltage. OLED external quantum efficiency (EQE) as a function of c) the injected current density and d) OLED luminance.

which can be exacerbated during solvent evaporation in solution processing techniques.

Following other reports of TTA-active devices using anthracene-based emitters,[24] host-free (non-doped) OLEDs were prepared using DPA emissive layers, but were found to crystalize before the devices could be measured.[24] Instead, 4,4′-bis(N-carbazolyl)-1,1′-biphenyl (CBP) was chosen as the host material due to its hole-transporting properties (complementary to the electron conductivity of anthracenes), its suitably high triplet energy compared to DPA (2.7 and 1.8 eV),[25] and in continuity with the above preliminary investigations in PVK films. Additional DPA devices using DPEPO hole-blocking or mCP electron-blocking layers (or thicker emissive layers) were found to have no appreciable impacts on performance or color, indicating recombination within the emissive layer rather than at either interface. Instead, consistently with the identified emitter aggregation in the more highly doped PVK films, we observe dramatic redshifts of the spiro-4-DPA device emission using 20 vol% or 80 vol% emissive layers, while DPA devices are entirely unimpacted (Figures S5 and S6, Supporting Information). The green emission in the 80% spiro-4-DPA devices was confirmed not to be a thermal decomposition product—initially suspected as the evaporation temperature of the spiro-4-DPA (≈400 °C) was much higher than lighter DPA (≈100 °C)—as subsequent re-fabrication of the 5% devices from the same crucible and material batch gave the same blue emission with no indication of contamination by a green-emissive component. Recovered evaporated material from inside the deposition chamber was also identical to the pristine material in NMR analysis (Figure S6, Supporting Information) and in powder and solution photoluminescence. Thus we ascribe the shift from blue to green electroluminescence to the spiro-4-DPA aggregate species, facilitated by higher deposition temperatures and as was observed to a lesser extent in PVK films and in powder (Figure S8, Supporting Information). Ultimately only for 5% doped devices the emission color was comparable for spiro-4-DPA and DPA, so although the external quantum efficiencies (EQE) retained the same trends at different concentrations as well, we consider only this composition in further analysis.

Figure 3 shows comparisons between the 5 vol% doped DPA and spiro-4-DPA devices. The electroluminescence spectra reflect the dye photoluminescence features (Figure 3a). The EQE performance of the spiro-4-DPA OLEDs is consistently better than that of the DPA devices, measured both with respect to current density (Figure 3c) and with respect to total brightness (Figure 3d). Having established that neither differences in device conductivity (Figure 3b) nor emitter ϕ_{pl} (from PVK films, Figure 2b) can explain the differences in device EQEs, we

© 2024 The Author(s). Advanced Optical Materials published by Wiley-VCH GmbH

21951071, 0, Downloaded from https://onlinelibrary.wiley.com/doi/10.1002/adom.202401597 by Universita Milano Biococca, Wiley Online Library on [23/10/2024]. See the Terms and Conditions (https://onlinelibrary.wiley.com/terms-and-conditions) on Wiley Online Library for rules of use; OA articles are governed by the applicable Creative Commons License

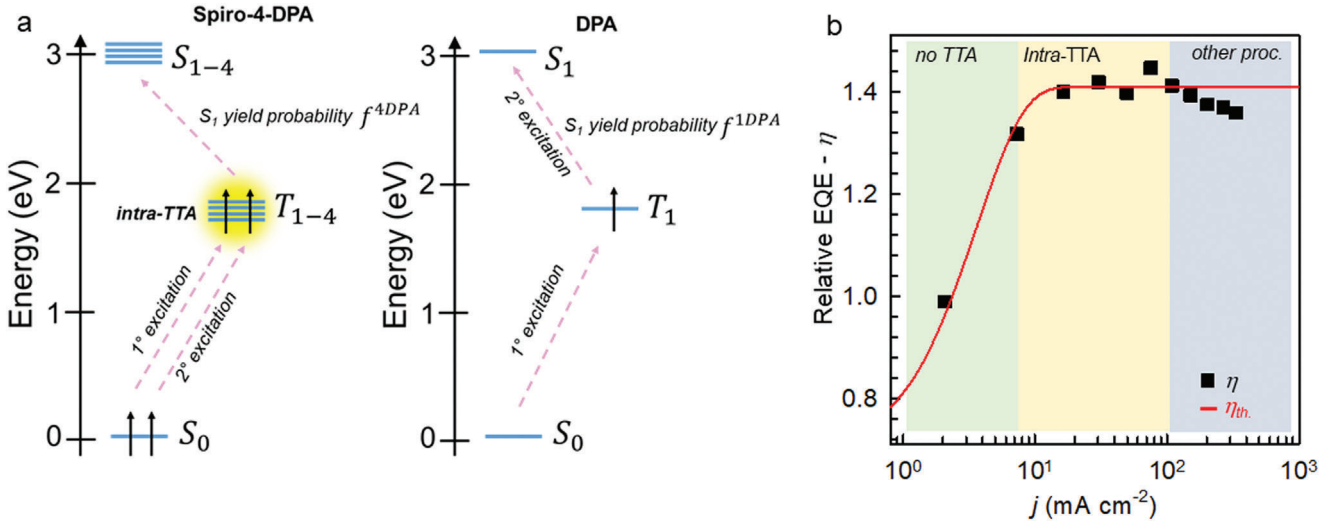

Figure 4. a) Sketch of the intra-TTA process active in the spiro-4-DPA and of the double excitation process of a single DPA molecule. f^{4DPA} and f^{1DPA} are the statistical probability to form an emissive singlet for the two processes, respectively. b) Measured (η) and predicted ($\eta_{th.}$) relative EQE as a function of j for the spiro-4-DPA 5% and DPA 5% blue emitting OLEDs. The $\eta_{th.}$ curve is calculated from the fit of the experimental EQEs data (Figure 3c) with Equation 2.

instead considered the possible contributions of inter- and intramolecular TTA.

In order to analyze the effect of intramolecular mechanisms, we propose a model to describe the bi-excitonic processes' contribution to OLED luminescence as a function of the injected current density j. We define the yield of the formation of the triplet-triplet pair state from injected charges, ϕ_{2T}, as

$$\phi_{2T}(j) = P(2 \mid \chi_T, \phi_{e-h}, \tau_T, j) \quad (1)$$

where χ_T is the statistical probability of forming the triplet molecular exciton upon charge recombination, with a specific value of 0.75. The function $P(2|\chi_T, \phi_{e-h}, \tau_T, j)$ is the cumulative probability of a site in the OLED emissive layer to hold two or more triplet excitons simultaneously, which are distributed following Poisson statistics (Section S5, Supporting Information). Practically, triplet excitons (proportional to j) are distributed into the OLED emissive layer sites (proportional to the dye concentrations, four times higher for DPA given the equal vol% loadings but differently sized dopants), and modulated by two contributions. On hand the exciton decay governed by the triplet lifetime τ_T, on the other hand their generation through charge capture and recombination to form molecular excitons ϕ_{e-h}. Notably, the coexistence of two excitons is the minimum condition where i) intra-TTA becomes active in the spiro-4-DPA, or ii) a DPA molecule in the triplet state T_1 can move up to a higher excited state through sequential absorption of a second T_1 exciton (**Figure 4a**).

In our OLEDs, the experimental EQE can be therefore expressed as the sum of singlet (S) and triplet (T) contributions as

$$\mathrm{EQE}(j) = \beta\phi_{pl}[\mathrm{S} + \mathrm{T}] = \beta\phi_{pl}\left[\phi_{e-h}\chi_s + 0.5f\phi_{2T}(j)\right] \quad (2)$$

where β is the efficiency of emission outcoupling and $\chi_S = 0.25$ is the statistical probability of forming singlet excited states upon charge recombination. The term $\phi_{e-h}\chi_s$ governs fluorescent OLEDs with no contribution from TTA or sequential triplet absorption. The emission generated by bi-excitonic processes is instead regulated by f, a parameter between 0 and 1 that represent the statistical probability that a singlet is generated upon interaction of two triplets, and by the formation of triplet pairs described by ϕ_{2T}. Upon the formation of a correlated triplet pair, the output state can be a singlet (with probability 1:9) or higher triplet (3:9) or a quintet (5:9). The output depends on several factors, among which the most relevant is energetic accessibility. For the system considered, the quintet state is not available energetically, while the energy of the T_2 state is only barely higher than $2\times T_1$. This implies that thermal energy can allow the conversion of the collisional complex T_1+T_1 to a T_2 state, with the loss of T_1 exciton. This implies the statistical intrinsic probability to have a singlet upconverted state upon TTA, i.e., the factor f, to have a maximum limit between 0.4 and 0.5.[19a,26–30] The factor 0.5 represents the pairwise conversion of two triplet excitons into a singlet.[31] Apart from $\phi_{2T}(j)$ and f, the factors in Equation 2 are either measured constants (ϕ_{pl}), or constants reasonably considered equal for both DPA and spiro-4-DPA devices (β, ϕ_{e-h}, χ_S,χ_T, Figures S3 and S4 (Supporting Information) for electrochemical properties). The $\phi_{2T}(j)$ yield is therefore the only factor that changes with the current density, and so we infer that this term alone controls the shape of the EQE curve as it rises to its maximum EQE. Beyond this maximum value we assume that multiexcitonic decay mechanisms (e.g., charge-exciton quenching) begin to dominate,[32] causing the EQE to fall (Figure 3c,d) for reasons unrelated to TTA. We also note that inter-TTA is mostly inactive in these devices considering the average inter-chromophore distances (≈3 vs ≈5 nm for DPA and spiro-4-DPA each at 5% loading, Section S5, Supporting Information).[33]

Fitting the EQE data to Equation 2 allows us to evaluate the shape of $\phi_{2T}(j)$ in the two devices (Figures S9 and S10, Supporting

© 2024 The Author(s). Advanced Optical Materials published by Wiley-VCH GmbH

21951071, 0, Downloaded from https://onlinelibrary.wiley.com/doi/10.1002/adom.202401597 by Universita Milano Bicocca, Wiley Online Library on [23/10/2024]. See the Terms and Conditions (https://onlinelibrary.wiley.com/terms-and-conditions) on Wiley Online Library for rules of use; OA articles are governed by the applicable Creative Commons License

Information). Moreover, to directly compare the two OLEDs we analyze therelative efficiency η defined as

$$\eta\ \left(f^{4DPA}, f^{1DPA}\right) = \frac{EQE_{4DPA}}{EQE_{DPA}} \quad (3)$$

where f^{1DPA} and f^{4DPA} are the statistical parameters for DPA and spiro-4-DPA respectively. This is due to the fact that the absolute values of f for the two devices cannot be independently determined without exact knowledge of β and ϕ_{e-h}. Nonetheless, fitting the experimental data with Equation 2 along with the known ϕ_{pl} values allows the f^{1DPA} and f^{4DPA} to be estimated.

Figure 4b shows how the experimental behavior of η (black squares) is nicely reproduced with the proposed model above (η_{th}, red solid line). Notably, fitting of the EQE curves for both systems yields very similar ϕ_{e-h} (Table S2, Supporting Information), in agreement with the comparable electronic properties of the two molecular systems (Figures S3 and S4, Supporting Information), and τ_T values in the milliseconds time scale as already demonstrated for DPA embedded in rigid polymeric matrixes (Figures S3 and S4 and Table S2, Supporting Information), but much slower decaying than in fluid solution.[19b,34]

For j values below 0.1 mA cm^{-2} the $\phi_{2T}(j)$ is low, thus the contribution of bi-excitonic processes to the OLED's emission is negligible. Between 1 and 80 mA cm^{-2} $\phi_{2T}(j)$ quickly reaches its maximum for both the spiro-4-DPA and DPA systems (Figure S10, Supporting Information). Notably, at the currents where the maximum EQEs, and therefore the maximum value of η, are observed, $\phi_{2T}(j)$ is unitary for both devices. We propose that in this regime it is the efficient intra-TTA channel that helps the spiro-4-DPA OLEDs to achieve a higher overall efficiency. The proposed modeling also affords a fitted $f^{4DPA} = 0.40$ for the spiro-4-DPA and $f^{1DPA} = 0.15$ for DPA, thus $f^{4DPA} \approx 2.7 \times f^{1DPA}$. This finding suggests that the fixed relative orientation of the spiro-4-DPA anthracene-like branches in the solid matrix is reasonably favorable for the formation of singlet molecular excitons upon TTA.[19b,28] Conversely, a subsequent double excitation of the DPA (or weak inter-TTA) seems to have a quite poor probability to relax to the emissive excited singlet configuration. Indeed in freely diffusing solution $f \approx 0.45$ is observed for the inter-TTA process when randomly oriented spiro-4-DPA and DPA molecules collide, which suggests that the performance of spiro-4-DPA in solid films is limited by the intrinsic properties of the anthracene chromophore rather than the geometry of the multi-chromophore scaffold.[21]

3. Conclusion

In summary, the intra-TTA active annihilator/emitter spiro-4-DPA is shown to outcompete isolated-chromophore reference material DPA in solid-state OLED applications. The efficiency enhancement of spiro-4-DPA is particularly evident a low injected current densities where intra-TTA dominates, and reaches a maximum enhancement ratio of +40% at 50 mA cm^{-2}. The obtained results suggest that this enhancement can be ascribed to the four-fold degenerate triplet states of the spiro-4-DPA system which, with respect to DPA, allow it to exploit an effective intra-TTA process to recover the energy stored in optically dark triplet exciton states especially at low injected current densities. Analysis of the OLED performance indicates that the intra-TTA process on the spiro-4-DPA in solid films has a similar spin-statistical probability to form singlets as the DPA molecule in fluid solution, with the later suffering significantly in dilute solid films. Ultimately the obtained results demonstrate that the use of intra-TTA active molecular designs is a very promising strategy to improve the performance of TTA OLEDs, but also for all TTA-based applications[6,35,36] by alleviating the requirements for triplet excitons to diffuse and form intermolecular pairs in the solid state.

4. Experimental Section

Optical Absorption and Photoluminescence Studies: UV–vis absorption spectra were recorded on a Cary Varian 50 spectrometer. Steady-state PL spectra were acquired with a with a nitrogen cooled charge coupled device (Spex ≈2000) coupled to a polychromator Triax 190 from J-Horiba. Steady-state fluorescence spectra were recorded using a 355 nm UV laser. Fluorescence emission intensity decay were recorded using a pulsed LED at 340 nm (3.65 eV, EP-LED 340 Edinburgh Instruments, pulse width of 700 ps). All spectra were corrected for the instrumental optical response. Solution photoluminescence quantum yield was obtained by relative methods (see Supporting Information), while the PVK film photoluminescence quantum yield has been measured using an integrating sphere with the de Mello method.[37]

Fabrication of PVK Dye Doped Films: The dye-loaded PVK films have been fabricated by drop casting on a quartz substrate a solution of PVK and dyes in dichloromethane.

OLED Fabrication: OLEDs were fabricated on patterned indium tin oxide (ITO) coated glass (VisionTek Systems) with a sheet resistance of 15 Ω per sq. Acetone and isopropanol sonicated substrates were oxygen-plasma cleaned and loaded into a Kurt J. Lesker Super Spectros deposition chamber, and both the small molecule and cathode layers were thermally evaporated at a pressure of below 10–7 mbar. The materials used for the transport and blocking layers were N,N-bis(naphthalen-1-yl)-N,N-bis(phenyl)benzidine (NPB, 40 nm) and 4,4′-(diphenylsilanediyl)bis(N,N-diphenylaniline) (TSBPA, 10 nm) as the hole injection/transport layers (HIL/HTL), CBP with codoped DPA or spiro-4-DPA as emissive layer (20 nm), followed by (1,3,5-benzinetriyl)-tris(1-phenyl-1-H-benzimidazole) (TPBi, 40 nm) as the ETL, lithium fluoride (LiF, 1 nm) as the EIL, and Al (100 nm) cathode through a shadow mask that defined 2 × 2, 2 × 4, and 4 × 4 mm pixels with the patterned ITO. Freshly evaporated devices were transferred into a calibrated 10 in. integrating sphere under ambient conditions. Electrical properties were measured using a source meter (Keithley 2400) simultaneously with emission spectrum and intensity with a calibrated fiber-coupled spectrometer (Ocean optics USB4000) sampling the inner surface of the sphere.

Supporting Information

Supporting Information is available from the Wiley Online Library or from the author.

Acknowledgements

A.M. and A.R. thank the project MUR -ANTHEM: "AdvaNced Technologies for Human-centrEd Medicine", ANTHEM – PNC0000003 CUP B53C22006670001. S.M. and L.B. thank the PRIN-PNR grant INPOWER no. P2022PXS5S-002. K.S. acknowledges the European Union's Horizon 2020 research and innovation programme for funding under the Marie Skłodowska-Curie grant agreement no. 812872 (TADFlife). A.M. acknowledges the EPSRC for funding under grant no. EP/T02240X/1. A.D. and A.M. thank the Durham-Uppsala Joint Seedcorn Fundfor financial support. The authors thank you Dr. Matteo Orfano for the preparation of the

© 2024 The Author(s). Advanced Optical Materials published by Wiley-VCH GmbH

RIGHTSLINK

21951071, 0, Downloaded from https://onlinelibrary.wiley.com/doi/10.1002/adom.202401597 by Universita Milano Bicocca, Wiley Online Library on [23/10/2024]. See the Terms and Conditions (https://onlinelibrary.wiley.com/terms-and-conditions) on Wiley Online Library for rules of use; OA articles are governed by the applicable Creative Commons License

luminescent PVK films and Prof. Riccardo Ruffo for discussions on the cyclovoltammetry experiments.

Open access publishing facilitated by Universita degli Studi di Milano-Bicocca, as part of the Wiley - CRUI-CARE agreement.

Conflict of Interest

The authors declare no conflict of interest.

Data Availability Statement

The data that support the findings of this study are available from the corresponding author upon reasonable request.

Keywords

blue OLEDs, conjugated chromophores, excitons, triplet–triplet annihilation, upconversion

Received: June 14, 2024
Revised: September 18, 2024
Published online:

[1] H. Uoyama, K. Goushi, K. Shizu, H. Nomura, C. Adachi, *Nature* **2012**, *492*, 234.
[2] a) A. Monkman, *ACS Appl. Mater. Interfaces* **2022**, *14*, 20463; b) I. A. Wright, A. Danos, S. Montanaro, A. S. Batsanov, A. P. Monkman, M. R. Bryce, *Chem. - Eur. J.* **2021**, *27*, 6545.
[3] D. Beery, T. W. Schmidt, K. Hanson, *ACS Appl. Mater. Interfaces* **2021**, *13*, 32601.
[4] C. Kerzig, O. S. Wenger, *Chem. Sci.* **2018**, *9*, 6670.
[5] Q. Dou, L. Jiang, D. Kai, C. Owh, X. J. Loh, *Drug Discovery Today* **2017**, *22*, 1400.
[6] S. N. Sanders, T. H. Schloemer, M. K. Gangishetty, D. Anderson, M. Seitz, A. O. Gallegos, R. C. Stokes, D. N. Congreve, *Nature* **2022**, *604*, 474.
[7] Y. Sasaki, M. Oshikawa, P. Bharmoria, H. Kouno, A. Hayashi-Takagi, M. Sato, I. Ajioka, N. Yanai, N. Kimizuka, *Angew. Chem., Int. Ed.* **2019**, *58*, 17827.
[8] W. Shockley, H. J. Queisser, *J. Appl. Phys.* **1961**, *32*, 510.
[9] a) D. Di, L. Yang, J. M. Richter, L. Meraldi, R. M. Altamimi, A. Y. Alyamani, D. Credgington, K. P. Musselman, J. L. MacManus-Driscoll, R. H. Friend, *Adv. Mater.* **2017**, *29*, 1605987; b) S. Izawa, M. Hiramoto, *Nat. Photonics* **2021**, *15*, 895; c) S. Izawa, M. Morimoto, K. Fujimoto, K. Banno, Y. Majima, M. Takahashi, S. Naka, M. Hiramoto, *Nat. Commun.* **2023**, *14*, 5494.
[10] J. U. Kim, I. S. Park, C.-Y. Chan, M. Tanaka, Y. Tsuchiya, H. Nakanotani, C. Adachi, *Nat. Commun.* **2020**, *11*, 1765.
[11] N. A. Kukhta, T. Matulaitis, D. Volyniuk, K. Ivaniuk, P. Turyk, P. Stakhira, J. V. Grazulevicius, A. P. Monkman, *J. Phys. Chem. Lett.* **2017**, *8*, 6199.
[12] A. J. Carrod, V. Gray, K. Börjesson, *Energy Environ. Sci.* **2022**, *15*, 4982.
[13] V. Gray, K. Moth-Poulsen, B. Albinsson, M. Abrahamsson, *Coord. Chem. Rev.* **2018**, *362*, 54.
[14] L. Huang, G. Han, *Nat. Rev. Chem.* **2024**, *8*, 238.
[15] S. Hisamitsu, N. Yanai, H. Kouno, E. Magome, M. Matsuki, T. Yamada, A. Monguzzi, N. Kimizuka, *Phys. Chem. Chem. Phys.* **2018**, *20*, 3233.
[16] A. R. Collins, B. Zhang, M. J. Bennison, R. C. Evans, *J. Mater. Chem. C* **2024**, *12*, 6310.
[17] F. Saenz, A. Ronchi, M. Mauri, R. Vadrucci, F. Meinardi, A. Monguzzi, C. Weder, *Adv. Funct. Mater.* **2021**, *31*, 2004495.
[18] F. Meinardi, M. Ballabio, N. Yanai, N. Kimizuka, A. Bianchi, M. Mauri, R. Simonutti, A. Ronchi, M. Campione, A. Monguzzi, *Nano Lett.* **2019**, *19*, 2169.
[19] a) W. Sun, A. Ronchi, T. Zhao, J. Han, A. Monguzzi, P. Duan, *J. Mater. Chem. C* **2021**, *9*, 14201; b) A. Olesund, V. Gray, J. Mårtensson, B. Albinsson, *J. Am. Chem. Soc.* **2021**, *143*, 5745.
[20] S. Sasaki, K. Goushi, M. Mamada, S. Miyazaki, K. Miyata, K. Onda, C. Adachi, *Adv. Opt. Mater.* **2024**, *12*, 2301924.
[21] S. Mattiello, S. Mecca, A. Ronchi, A. Calascibetta, G. Mattioli, F. Pallini, F. Meinardi, L. Beverina, A. Monguzzi, *ACS Energy Lett.* **2022**, *7*, 2435.
[22] a) L. G. Franca, Y. Long, C. Li, A. Danos, A. Monkman, *J. Phys. Chem. Lett.* **2021**, *12*, 1490; b) L. G. Franca, A. Danos, A. Monkman, *J. Mater. Chem. C* **2022**, *10*, 1313; c) L. G. Franca, A. Danos, A. Monkman, *J. Phys. Chem. Lett.* **2023**, *14*, 2764.
[23] a) T. Ogawa, N. Yanai, S. Fujiwara, T.-Q. Nguyen, N. Kimizuka, *J. Mater. Chem. C* **2018**, *6*, 5609; b) E. Radiunas, M. Dapkevičius, S. Raišys, K. Kazlauskas, *Phys. Chem. Chem. Phys.* **2022**, *24*, 24345.
[24] R. Ieuji, K. Goushi, C. Adachi, *Nat. Commun.* **2019**, *10*, 5283.
[25] M. Colella, A. Danos, A. P. Monkman, *J. Phys. Chem. C* **2019**, *123*, 17318.
[26] R. E. Merrifield, *J. Chem. Phys.* **1968**, *48*, 4318.
[27] A. Monguzzi, J. Mezyk, F. Scotognella, R. Tubino, F. Meinardi, *Phys. Rev. B* **2008**, *78*, 195112.
[28] J. Mezyk, R. Tubino, A. Monguzzi, A. Mech, F. Meinardi, *Phys. Rev. Lett.* **2009**, *102*, 087404.
[29] S. Hoseinkhani, R. Tubino, F. Meinardi, A. Monguzzi, *Phys. Chem. Chem. Phys.* **2015**, *17*, 4020.
[30] L. Vaghi, F. Rizzo, J. Pedrini, A. Mauri, F. Meinardi, U. Cosentino, C. Greco, A. Monguzzi, A. Papagni, *Photochem. Photobiol. Sci.* **2022**, *21*, 913.
[31] a) Y. Zhou, F. N. Castellano, T. W. Schmidt, K. Hanson, *ACS Energy Lett.* **2020**, *5*, 2322; b) A. Ronchi, A. Monguzzi, *Chem. Phys. Rev.* **2022**, *3*, 041301.
[32] H. van Eersel, P. A. Bobbert, R. A. J. Janssen, R. Coehoorn, *Appl. Phys. Lett.* **2014**, *105*, 143303.
[33] D. L. Dexter, *J. Chem. Phys.* **1953**, *21*, 836.
[34] A. Monguzzi, M. Mauri, M. Frigoli, J. Pedrini, R. Simonutti, C. Larpent, G. Vaccaro, M. Sassi, F. Meinardi, *J. Phys. Chem. Lett.* **2016**, *7*, 2779.
[35] P. Bi, T. Zhang, Y. Guo, J. Wang, X. W. Chua, Z. Chen, W. P. Goh, C. Jiang, E. E. M. Chia, J. Hou, L. Y., *Nat. Commun.* **2024**, *15*, 5719.
[36] X. Hu, D. Rigamonti, I. Villa, L. Pollice, M. Mauri, A. D. Molin, M. Tardocchi, F. Meinardi, C. Weder, A. Monguzzi, *Adv. Mater.* **2024**, *36*, 2400443.
[37] J. C. de Mello, H. F. Wittmann, R. H. Friend, *Adv. Mater.* **1997**, *9*, 230.

© 2024 The Author(s). Advanced Optical Materials published by Wiley-VCH GmbH

RIGHTSLINK

21951071, 0, Downloaded from https://onlinelibrary.wiley.com/doi/10.1002/adom.202401597 by Universita Milano Bicocca, Wiley Online Library on [23/10/2024]. See the Terms and Conditions (https://onlinelibrary.wiley.com/terms-and-conditions) on Wiley Online Library for rules of use; OA articles are governed by the applicable Creative Commons License